

## MAJOR ARTICLE

# Linezolid population pharmacokinetic model in plasma and cerebrospinal fluid among patients with tuberculosis meningitis

Noha Abdelgawad,<sup>1†</sup> Sean Wasserman,<sup>2,3†</sup> Mahmoud Tareq Abdelwahab,<sup>1</sup> Angharad Davis,<sup>2,5,6</sup> Cari Stek,<sup>2</sup> Lubbe Wiesner,<sup>1</sup> John Black,<sup>7</sup> Graeme Meintjes,<sup>2,8</sup> Robert J. Wilkinson,<sup>2,4,5,9</sup> Paolo Denti<sup>1</sup>

<sup>1</sup>Division of Clinical Pharmacology, Department of Medicine, University of Cape Town, Observatory 7925, South Africa; <sup>2</sup>Centre for Infectious Diseases Research in Africa, Institute of Infectious Disease and Molecular Medicine, University of Cape Town, Observatory 7925, South Africa; <sup>3</sup> Institute for Infection and Immunity, St George's University of London, United Kingdom; <sup>4</sup> Division of Infectious Diseases and HIV Medicine, Department of Medicine, University of Cape Town, Observatory 7925, South Africa; <sup>5</sup> The Francis Crick Institute, London NW1 1AT, United Kingdom; <sup>6</sup> Faculty of Life Sciences, University College London, WC1E 6BT, United Kingdom; <sup>7</sup> Department of Medicine, Walter Sisulu University, Mthatha, South Africa; <sup>8</sup> Department of Medicine, University of Cape Town, Observatory 7925, South Africa; <sup>9</sup> Department of infectious Diseases, Imperial College London W12 0NN, United Kingdom

**Background:** Linezolid is evaluated in novel treatment regimens for tuberculous meningitis (TBM). Linezolid pharmacokinetics have not been characterized in this population, particularly in cerebrospinal fluid (CSF) where exposures may be affected by changes in protein concentration. Linezolid co-administration with high-dose rifampicin, has also not been studied. We aimed to characterize linezolid plasma and CSF pharmacokinetics in adults with TBM.

**Methods:** In LASER-TBM pharmacokinetic-substudy, the intervention groups received high-dose rifampicin (35mg/kg) plus linezolid 1200mg/day for 28days, then reduced to 600mg/day.

†Contributed equally to this manuscript

#Address correspondence to Noha Abdelgawad, K45 Old Main Building, Groote Schuur Hospital Observatory, Cape Town, 7925, South Africa, phone: +27 21 404 7719, email: abdnoh001@myuct.ac.za

© The Author(s) 2023. Published by Oxford University Press on behalf of Infectious Diseases Society of America. This is an Open Access article distributed under the terms of the Creative Commons Attribution License (<https://creativecommons.org/licenses/by/4.0/>), which permits unrestricted reuse, distribution, and reproduction in any medium, provided the original work is properly cited.

Plasma sampling was done on day 3 (intensive) and on day 28 (sparse). A lumbar CSF sample was obtained on both visits.

**Results:** 30-participants, median(min-max) age and weight of 40(27–56)years and 58(30–96)kg, contributed 247 plasma and 28 CSF observations. Plasma pharmacokinetics was described by one-compartment model with first-order absorption and saturable elimination. Maximal clearance was 7.25L/h, and  $K_m$  was 27.2mg/L. Rifampicin co-treatment duration did not affect linezolid pharmacokinetics. CSF-Plasma partitioning correlated with CSF total-protein upto 1.2g/L where the partition-coefficient reached maximal value of 37%. Plasma-CSF equilibration half-life was ~3.5hours

**Conclusion:** Linezolid was readily detected in CSF despite high-dose rifampicin co-administration. These findings support continued clinical evaluation of linezolid plus high-dose rifampicin for the treatment of TBM in adults.

**Keywords:** Population pharmacokinetics, Tuberculosis Meningitis, Linezolid, Cerebrospinal fluid, Modelling & Simulation

## INTRODUCTION

Tuberculous meningitis (TBM) is the most fatal and debilitating form of tuberculosis with a particularly high burden among people living with HIV [1]. One reason for severe outcomes is that the current treatment regimen for TBM is based on treatment for pulmonary TB, and may result in suboptimal central nervous system (CNS) concentrations [2]. Drugs targeted at TBM should cross several barriers to reach the site of disease, including the blood-brain barrier (BBB) and the blood-cerebrospinal fluid barrier (BCSFB) that separate the systemic circulation from their site of action in the CNS. These barriers pose a therapeutic challenge by limiting entry of drugs into the CNS. Moreover, disease-related changes in BBB permeability and dynamic changes in protein concentrations may have important implications for drug penetration into the brain [3].

Linezolid, an oxazolidinone antibiotic, is highly effective for the treatment of drug-resistant pulmonary TB. Linezolid is also used to treat Gram-positive bacterial infections in the CNS [4–6], where good drug penetration has been documented, making it an attractive candidate for TBM treatment [7–9]. Small observational studies have shown improved clinical parameters with linezolid use in children and adults with TBM [10,11]. Based on these encouraging observations, linezolid is being investigated as part of intensified antibiotic therapy in several clinical trials for TBM [12].

Specific features of TBM may influence the pharmacokinetics (PK) of linezolid, with potential implications for safety and efficacy, given its narrow therapeutic window. These include host factors (such as body size) and disease factors, including CSF protein concentrations and BBB

permeability. Also, clinical trials provide linezolid along with high-dose rifampicin in TBM treatment regimens. As a potent inducer of the cytochrome P450 system and upregulator of drug transporters [13], rifampicin could potentially affect the PK of linezolid. Studies in healthy volunteers and pulmonary TB have shown a moderate reduction in linezolid exposure when co-administered with standard dose rifampicin [14,15]. The impact on site of disease (CSF) concentrations and clinical implications of this pharmacokinetic interaction is unknown but could theoretically lead to suboptimal treatment or the development of antimicrobial resistance.

The objectives of this analysis were to describe the PK of linezolid in plasma and CSF of adults with TBM, to explore the effect of high-dose rifampicin on linezolid PK, evaluate covariate effects on plasma and CSF drug levels, and simulate exposures for optimized dosing strategies.

## METHODOLOGY

### Study data

This was a sub-study of LASER-TBM [16], a phase IIb, open-label trial that evaluated safety and PK of intensified antibiotic therapy in adults with HIV and TBM [12]. Participants were enrolled from 4 public hospitals in Cape Town and Gqeberha, South Africa, and randomized to study interventions within 5 days of starting antituberculosis treatment. The standard of care (control) group received fixed-dose combination oral tablets (rifampicin 10 mg/kg, isoniazid 5 mg/kg, pyrazinamide 25 mg/kg, and ethambutol 15 mg/kg) according to World Health Organization (WHO) weight bands. Participants allocated to experimental groups were administered the standard regimen with a higher dose of rifampicin (35 mg/kg in total, using bespoke weight bands [17]) and linezolid for 56 days (1200 mg once daily for the first 28 days, then reduced to 600 mg once daily) with or without aspirin. All participants received adjunctive dexamethasone.

Pharmacokinetic sampling visits were scheduled on Day 3 ( $\pm 2$  days) and Day 28 ( $\pm 2$  days) after study entry. At the Day 3 visit, plasma was collected at pre-dose, 0.5, 1, 2, 3, 6, 8-10, and 24 hours post-dose (intensive) and on Day 28 at pre-dose, 2-, and 4-hours post-dose (sparse). Sparse sampling was performed on Day 3 for participants who declined intensive sampling or for whom intensive sampling could not be done. One lumbar CSF sample was collected at each pharmacokinetic sampling visit, with sample timing randomized to intervals of 1-3, 3-6, 6-10, and 24 hours after dosing. Clinical information was collected, and full blood count and serum chemistry were obtained at each visit. Total protein, albumin, and glucose were measured in CSF samples.

Linezolid plasma and CSF concentrations were measured in the Division of Clinical Pharmacology at the University of Cape Town. The plasma assay summary has been described previously [18]. Cholesterol and 4-beta hydroxy cholesterol (4 $\beta$ -OHC) were also measured in pre-dose plasma samples collected on both PK visits. 4 $\beta$ -OHC is a metabolite of cholesterol

formed by CYP3A4 and the ratio between its concentration and that of cholesterol is used as a marker of CYP3A4/5 endogenous activity [19]. Additionally, the unbound concentration of linezolid in plasma was quantified in a subset of samples to estimate the degree of plasma protein binding. Details of analytical assays are outlined in the supplementary file.

Informed consent was obtained from all participants or their proxies. The study was approved by the University of Cape Town Human Research Ethics Committee (UCT HREC reference: 293/2018), Walter Sisulu University (HREC reference: 012/2019), and the South African Health Products Regulatory Authority (reference number 20180622). The trial is registered on [clinicaltrials.gov](https://clinicaltrials.gov) (NCT03927313).

### Pharmacokinetic modelling

Nonlinear mixed-effects modelling was used to create a population PK model describing linezolid PK in both plasma and lumbar CSF. The model was developed sequentially; first describing plasma linezolid and then including CSF concentrations.

For the plasma PK, we tested one- and two-compartment disposition models with linear or saturable elimination and first-pass effect. The CSF concentrations were described using a hypothetical effect compartment linked to the central (plasma) compartment, which estimates the first-order equilibration rate constant of linezolid between the central and the effect compartments ( $k_{plasma-CSF}$ ) and the pseudo-partition coefficient ( $PPC$ ). Further details on modelling approach are available in the supplementary file.

Following the development of the structural model, we tested the effect of potential covariates including creatinine clearance (calculated with the Cockcroft-Gault equation [23]), age, study visit, duration of concomitant rifampicin treatment, study site, and treatment arm. For the CSF PK parameters  $PPC$  and  $k_{plasma-CSF}$ , we also tested the effect of CSF total protein, albumin, and glucose concentrations. The precision of the parameter estimates of the final model, expressed as 95% confidence intervals and %RSE, was assessed using sampling importance resampling (SIR) [24].

In the plasma samples with matched free and total linezolid concentrations available, the free concentrations were regressed against the total concentration with intercept of zero using Deming regression [25,26]. The fraction unbound ( $f_u$ ) was estimated from the slope of the regression line.

### Simulations

The model-derived area under the concentration-time curve from time 0 to 24 hours post-dose ( $AUC_{0-24h}$ ) and the concentration at 24 hours post-dose ( $C_{24h}$ ) were calculated for the available profiles. Monte Carlo simulations ( $n=10,000$ ) were performed using final model parameters to simulate concentration-time profiles in plasma and CSF following daily linezolid doses of 600

mg or 1200 mg at steady-state for a typical participant with median FFM of 45 kg and CSF protein of 0.995 mg/mL.

## RESULTS

### Study data

Thirty participants underwent PK sampling on the first PK visit on day 3 of the study and 18 participants had PK sampling at the second PK visit on day 28, one of whom was excluded from this analysis because all 3 samples were BLQ (later confirmed to have missed dosing). Reasons for missing the second PK visit included death, interrupting linezolid dose due to adverse events, or withdrawing consent. There were 247 plasma concentrations (6 were BLQ, 2.43%) and 28 CSF concentrations (7 were BLQ, 25%) available for PK modeling. All participants were receiving linezolid 1200 mg daily at the first PK visit; on day 28, 13 received 1200 mg and 4 received 600 mg. Baseline clinical characteristics are summarized in **Table 1**. Median CD4 count was 137 cells/mm<sup>3</sup> (range 2 to 890). Median duration on rifampicin therapy was 5 days (range 0 – 7) at the Day 3 PK visit and 30 days (range 27 – 38) at the Day 28 visit. Median CSF total protein concentrations decreased from 1.46 g/L (range 0.31 – 54.7) at Day 3 to 0.75 g/L (range 0.22 – 2.19) at Day 28.

### Pharmacokinetic modelling

The plasma PK of linezolid was best characterized by a one-compartment disposition model, saturable elimination with Michaelis–Menten, and first-order absorption preceded by a chain of transit compartments. Saturable elimination resulted in a better model fit than linear elimination (dOFV = -9.03, *p*-value = 0.00205, df = 1). A schematic diagram of the model is shown in **Figure 1**. Two-compartment disposition was tested but did not result in a significant improvement of fit. Maximal clearance (*CL*<sub>max</sub>) and volume of distribution (*V*) were allometrically scaled using FFM (drop in objective function value (dOFV) = -30, compared to dOFV = -7.7 when using total body weight). In a typical participant (median FFM 45 kg) the value of maximal clearance (*CL*<sub>max</sub>) was 7.25 L/h, the Michaelis-Menten constant (*K*<sub>m</sub>), which is a parameter that governs saturable hepatic elimination and represents the linezolid concentration at which half the *CL*<sub>max</sub> is reached, was 27.2 mg/L, and the volume of distribution (*V*) was 40.8 L. The inclusion of between-visit variability in *CL*<sub>max</sub> improved the model fit, but no systematic increase or decrease with time on treatment was observed. Longitudinal changes in clearance were explored by testing auto-inhibition and duration of rifampicin co-treatment, but no significant effect was found for either. We also could not find any effect when testing the ratio of 4β-OHC to cholesterol, creatinine clearance, or age on *CL*<sub>max</sub> and bioavailability (*F*). The final parameter estimates are presented in **Table 2**. A visual predictive check showing adequate model fit is depicted in **Figure S1** in the supplementary file.

The CSF concentrations were linked to the plasma concentrations with an equilibration half-life of 3.5 hours (95% confidence interval, 2.04 - 8.16) and the steady-state equilibrium ratio (*PPC*), indicating the relative amount of linezolid exposure in CSF, which was dependent on CSF protein levels. The *PPC*-CSF protein relationship was described using a piece-wise linear (broken-stick) function, where the *PPC* increased with higher CSF protein levels until a maximal CSF protein value where the *PPC* plateaued (i.e., a maximal *PPC* value). The breakpoint was estimated, while the slope (i.e., the change in *PPC* per change in CSF protein) was calculated from the breakpoint and the intercept (minimum *PPC*) which was fixed to be 0 to prevent the estimation of negative values of *PPC* which are physiologically unfeasible. For each 0.1 mg/mL increase in CSF protein, we found an increase of 3% in *PPC* up to 1.18 mg/mL of CSF protein, after which the *PPC* reached a maximal value of 0.365 (95% CI, 0.238 – 0.566) (**Figure 2**). Both CSF protein and CSF albumin were found to correlate significantly with *PPC*; however, the two are highly positively correlated. Only CSF protein was included in the final model because it resulted in a more significant drop in OFV and because albumin is a component of the proteins measured.

The regression plots of linezolid free concentrations versus total concentration (mg/L) and of linezolid *fu* versus total linezolid concentrations (mg/L) are shown in **Figures S3** and **S4** in the supplementary file. There was no apparent trend of changing *fu* across the observed total linezolid concentration range.

### Simulations

The simulated plasma and CSF concentration time profiles for the typical participant in our cohort following a once daily dose of either 600 mg or 1200 mg linezolid are depicted in **Figure 2** and model-derived individual values for the steady-state  $AUC_{0-24h}$  and trough concentrations are summarized in **Table 3**.

## DISCUSSION

Linezolid is being evaluated in several clinical trials as part of enhanced antimicrobial therapy for TBM. This is based on limited clinical evidence from small observational studies in TBM [10,11] and reports of successful use in gram-positive CNS infection. However, there is scarce information on linezolid exposure in the CSF, especially among patients with TBM, a presumed requirement for clinical efficacy in this condition. We characterized the PK of linezolid in plasma and CSF from a cohort of South African patients with HIV-associated TBM. The extent of linezolid penetration into the CSF was ~30% on average of plasma exposure and correlated with CSF protein concentrations – CSF penetration was higher in participants with higher CSF protein, reaching a maximal value of ~37%. Co-administration with high-dose rifampicin (35 mg/kg/day), when comparing the duration on rifampicin treatment on day 3 versus day 28 did not have a significant effect on the PK of linezolid.

Several prior studies may help to contextualize our findings. A recent observational study reported CSF linezolid concentrations from 17 TBM patients (only one with HIV) who received linezolid 600 mg daily [27]. The median CSF concentrations were 0.90 mg/L and 3.14 mg/L and the CSF/serum ratios were 0.25 and 0.59 at 2- and 6-hours post-dose, respectively. CSF linezolid concentrations have also been reported from two small cohorts of neurosurgical patients receiving 600 mg linezolid intravenously every 12 hours. In the smaller study ( $n = 7$ ) the mean observed CSF-to-plasma AUC ratio was 0.565 ( $n = 7$ ), the mean ( $\pm$ standard deviation)  $AUC_{0-\infty}$  after the first dose was 37.7 ( $\pm 23.9$ ) mg·h/L and  $AUC_{0-12h}$  after the fifth dose was 53.7 ( $\pm 50.3$ ) mg·h/L. In the slightly larger study ( $n = 14$ ) mean observed CSF-to-plasma AUC ratio was 0.66 and mean ( $\pm$ standard deviation) AUC in CSF was 101  $\pm$ 59.6 mg.h/L [28,29]. Direct comparison is limited because of differences in population (HIV status, disease type and severity), dosing and administration, and drug assays. CSF/plasma concentration and AUC ratios should be cautiously interpreted in these prior studies [27–29] since observed CSF and plasma concentrations were compared at the same timepoints, not accounting for delay in distribution between the plasma and CSF. Despite having access to only a single CSF sample per visit (due to the invasive nature of lumbar puncture), using a model-based approach allowed us to describe the time course for linezolid entry into CSF. The limitation of sparse CSF sampling in our study was further mitigated by randomizing participants to different sampling times so that CSF samples could be obtained over the full dosing interval. Another limitation is the relatively high proportion of BLQ CSF samples, which gives a high variability in the observed CSF concentrations that is reflected in the proportional error estimate for the CSF observations. To test the effect of these samples on our analysis, we conducted a sensitivity analysis after excluding the BLQ samples. Excluding the BLQ samples mainly affected the estimate of the proportional error – which decreased but did not affect the estimates of the pseudo-partition coefficient and the equilibration half-life. Additionally, we performed a parametric bootstrap (stochastic simulation and estimation, SSE) which yielded uncertainty values in line with the values obtained from SIR, thus corroborating our confidence in the results [30].

Other studies have also reported a relationship between the levels of CSF total protein (or albumin) and antituberculosis drugs in TBM [31,32]. In a pediatric population there was a linear relationship between log-transformed CSF protein concentration and the CSF penetration of rifampicin, with a 63% increase in the penetration coefficient for every 10-fold change in protein levels [31]. In another pediatric TBM cohort, an exponential function was used to describe the relationship between CSF protein concentrations and the partition coefficient of rifampicin where an increase of 1 g/L in CSF protein concentration resulted in a 1.28-fold increase in the partition coefficient [32].

There are two plausible, potentially overlapping, explanations for our finding of a correlation between CSF protein levels and extent of CSF linezolid partitioning. In a healthy state, the BCSFB is intact and only a small fraction of plasma proteins can enter into the CNS, leaving only unbound drug fraction available for penetration into this compartment [7]. Inflammation

associated with TB meningitis may increase BCSFB permeability causing both plasma protein and total drug concentrations to be higher in the CSF. Another possible explanation for this relationship is higher endogenous CSF protein production from local inflammation leading to alterations in CSF drug binding kinetics and higher concentrations of total drug in TBM. Quantification of free drug CSF concentrations may help to further delineate CSF protein-drug relationships.

Linezolid is provided with high dose rifampicin (35 mg/kg/day) in ongoing efficacy trials for TBM. Because of prior reports of a drug-drug interaction between rifampicin and linezolid, plus the likelihood of a rifampicin dose effect on metabolizing enzyme activity [33] which could affect the linezolid plasma exposure and hence the CSF exposure, we investigated a potential effect of rifampicin on linezolid PK. In our study, there was no control group of participants who received only linezolid without rifampicin to clearly identify a drug-drug interaction. However, estimated linezolid clearance in our cohort was comparable to that reported from patients receiving linezolid for drug-resistant pulmonary TB without concomitant rifampicin. In addition, since the maximal cytochrome (CYP) P450 induction effect of rifampicin occurs after at least a week [34], we investigated the effect of the duration of rifampicin therapy (rather than rifampicin co-administration as categorical covariate) on linezolid PK, and could not detect any significant trends. Furthermore, we found no relationship between  $4\beta$ -OHC:cholesterol or  $4\beta$ -OHC alone (as predictive biomarker of enzyme induction by rifampicin) and linezolid clearance or bioavailability. Our data indicate that even if rifampicin had an effect on linezolid exposures, it is unlikely to be clinically relevant.

In contrast to our findings, other smaller studies among healthy volunteers and non-TB patients have demonstrated a reduction in linezolid exposure when co-administered with rifampicin [14,35–37]. This interaction has been variously attributed to either a large increase in the expression of the CYP3A4 isoenzyme that typically has a small contribution to linezolid clearance [14] or to increased upregulation of linezolid intestinal secretion by rifampicin induction of P-glycoprotein (P-gp) [37]. There is no definitive evidence that linezolid is a substrate of P-gp, plus it is mainly (~68%) metabolized in the liver via morpholine ring oxidation, which is independent of the CYP450 system, with the remainder excreted unchanged via the kidneys [14].

As reported for pulmonary TB patients, saturable elimination was observed at higher linezolid plasma concentrations, resulting in non-linear PK [38]. Despite subtle differences in Michaelis-Menten elimination kinetics ( $K_m$ ) our estimates for  $CL_{max}$  and  $V$  are in line with previously published linezolid models [38–43]. Prior models based on data from non-TB [44] and pulmonary TB patients [45], included an empirical inhibition compartment to describe concentration- and time-dependent autoinhibition of elimination. We also tested this approach, but it did not result in a better model fit for our data, and clearance values estimated by these models are similar to ours.



An overview of these models and a comparison with the current work is summarized in **Table S1** in the supplementary file.

Our analysis had several limitations. First, the sparse plasma sampling (3 samples) performed during the 2<sup>nd</sup> PK visit does not allow for robust estimation of the non-linearity in clearance, especially since only 7 participants were on the reduced dose (600 mg). However, the model fit improved significantly ( $p$ -value < 0.001) when including saturation of clearance with higher concentrations, supporting this conclusion. Secondly, a limitation of the *PPC*-CSF protein relationship in our model is that the minimum *PPC* was fixed to 0 – meaning no linezolid enters the CSF - to prevent the estimation of negative values of *PPC* which are physiologically implausible. However, a CSF protein value of 0 is also not observed in people where it varies between 0.2% and 0.5% of the total protein concentration of blood [46]. It is considered that 80% of CSF proteins originate in blood and that CSF proteins are diluted in a molecule-size-dependent concentration gradient [47]. Finally, we did not undertake simulations to estimate probability of target attainment because a PK efficacy target is not established for TBM. While our simulations do suggest that 1200 mg daily dosing will achieve linezolid concentrations above the critical concentration MIC for *M. tuberculosis*, it is important to note that this putative efficacy target is established in-vitro under conditions that are completely different from CSF. Additionally, drug protein binding (and relative free fraction of active drug) in the CSF is unknown.

In conclusion, we successfully developed a population PK model for linezolid among adults with HIV-associated TBM, demonstrating that linezolid penetrates into the CSF, a surrogate compartment for site of disease in TBM, at potentially therapeutic concentrations, even with concomitant use of high-dose rifampicin. More investigations on the CSF protein binding dynamics of linezolid are required to better understand its CSF partition. These findings support continued clinical evaluation of linezolid together with rifamycins for the treatment of TBM in adults. Our model provides a platform that can be used for exploring alternative linezolid dosing strategies in TBM once effective and safe treatment targets are established for this condition.

**Conflict of interest:** All authors declare no competing interests for this work.

**Funding:** SW was supported by the National Institutes of Health (K43TW011421 and U01AI170426). MA received training in research that was supported by the Fogarty International Center of the National Institutes of Health under Award Number D43 TW010559. This work was supported by the Wellcome through core funding from the Wellcome Centre for Infectious Diseases Research in Africa (203135/Z/16/Z). AGD was supported by a UCL Wellcome Trust PhD Programme for Clinicians Fellowship (award number 175479). RJW receives support from the Francis Crick Institute which is funded by Wellcome (CC2112), Cancer Research UK (CC2112) and UK Research and Innovation (CC2112). He also receives support from NIH (R01145436) and Meningitis Now. The University of Cape Town Clinical PK Laboratory is supported in part via the Adult Clinical Trial Group (ACTG), by the National

Institute of Allergy and Infectious Diseases (NIAID) of the National Institutes of Health under award numbers UM1 AI068634, UM1 AI068636, and UM1 AI106701; as well as the Infant Maternal Pediatric Adolescent AIDS Clinical Trials Group (IMPACT), funding provided by National Institute of Allergy and Infectious Diseases (U01 AI068632), The Eunice Kennedy Shriver National Institute of Child Health and Human Development, and National Institute of Mental Health grant AI068632. The content is solely the responsibility of the authors and does not necessarily represent the official views of the sponsors. The funders had no role in study design, data collection and analysis, decision to publish, or preparation of the manuscript. For the purpose of Open Access, the authors have applied a CC-BY public copyright license to any Author Accepted Manuscript version arising from this submission.

**Acknowledgments:** Computations were performed using facilities provided by the University of Cape Town's ICTS High Performance Computing team: <https://ucthpc.uct.ac.za/>. Study data were collected and managed using REDCap (Research Electronic Data Capture) tools hosted at the University of Cape Town. REDCap is a secure, web-based software platform designed to support data capture for research studies [48,49].

## REFERENCES

1. Dodd PJ, Yuen CM, Sismanidis C, Seddon JA, Jenkins HE. The global burden of tuberculosis mortality in children: a mathematical modelling study. *Lancet Glob Heal* [Internet]. Elsevier; **2017** [cited 2021 Oct 4]; 5(9):e898–e906. Available from: <https://linkinghub.elsevier.com/retrieve/pii/S2214109X17302899>
2. Wasserman S, Davis A, Wilkinson RJ, Meintjes G. Key considerations in the pharmacotherapy of tuberculous meningitis. *Expert Opin Pharmacother* [Internet]. Taylor & Francis; **2019** [cited 2022 Oct 2]; 20(15):1791–1795. Available from: <https://www.tandfonline.com/doi/abs/10.1080/14656566.2019.1638912>
3. Pardridge WM. Drug transport across the blood–brain barrier. *J Cereb Blood Flow Metab* [Internet]. SAGE Publications; **2012** [cited 2022 Jul 26]; 32(11):1959. Available from: </pmc/articles/PMC3494002/>
4. Pintado V, Pazos R, Jiménez-Mejías ME, et al. Linezolid for therapy of Staphylococcus aureus meningitis: a cohort study of 26 patients. *Infect Dis (London, England)* [Internet]. Taylor & Francis; **2020** [cited 2022 Oct 24]; 52(11):808–815. Available from: <https://www.tandfonline.com/doi/abs/10.1080/23744235.2020.1789212>
5. Beer R, Pfausler B, Schmutzhard E. Management of nosocomial external ventricular drain-related ventriculomeningitis. *Neurocrit Care*. **2009**; 10(3):363–367.
6. Hoefnagel D, Dammers R, Laak-Poort MP Ter, Avezaat CJJ. Risk factors for infections related to external ventricular drainage. *Acta Neurochir (Wien)*. **2008**; 150(3):209–214.
7. Nau R, Sörgel F, Eiffert H. Penetration of Drugs through the Blood-Cerebrospinal Fluid/Blood-Brain Barrier for Treatment of Central Nervous System Infections. *Clin Microbiol Rev* [Internet]. *Clin Microbiol Rev*; **2010** [cited 2022 Apr 4]; 23(4):858–883. Available from: <https://pubmed.ncbi.nlm.nih.gov/20930076/>

8. Rupprecht TA, Pfister H-W. Clinical experience with linezolid for the treatment of central nervous system infections. *Eur J Neurol* [Internet]. **2005**; 12(7):536–542. Available from: <https://onlinelibrary.wiley.com/doi/10.1111/j.1468-1331.2005.01001.x>
9. Villani P, B. Regazzi M, Marubbi F, et al. Cerebrospinal Fluid Linezolid Concentrations in Postneurosurgical Central Nervous System Infections. *Antimicrob Agents Chemother* [Internet]. **2002**; 46(3):936–937. Available from: <https://journals.asm.org/doi/10.1128/AAC.46.3.936-937.2002>
10. Sun F, Ruan Q, Wang J, et al. Linezolid manifests a rapid and dramatic therapeutic effect for patients with life-threatening tuberculous meningitis. *Antimicrob Agents Chemother* [Internet]. American Society for Microbiology; **2014** [cited 2022 Apr 7]; 58(10):6297–6301. Available from: <https://journals.asm.org/doi/10.1128/AAC.02784-14>
11. Li H, Lu J, Liu J, Zhao Y, Ni X, Zhao S. Linezolid is Associated with Improved Early Outcomes of Childhood Tuberculous Meningitis. *Pediatr Infect Dis J* [Internet]. **2016** [cited 2022 Apr 7]; 35(6):607–610. Available from: <https://pubmed.ncbi.nlm.nih.gov/26901441/>
12. Davis AG, Wasserman S, Stek C, et al. A phase 2A trial of the safety and tolerability of increased dose rifampicin and adjunctive linezolid, with or without aspirin, for HIV-associated tuberculous meningitis (The LASER-TBM Trial). *Clin Infect Dis* [Internet]. *Clin Infect Dis*; **2022** [cited 2023 Mar 22]; . Available from: <https://pubmed.ncbi.nlm.nih.gov/36482216/>
13. Finch CK, Chrisman CR, Baciewicz AM, Self TH. Rifampin and Rifabutin Drug Interactions: An Update. *Arch Intern Med* [Internet]. American Medical Association; **2002** [cited 2022 Oct 26]; 162(9):985–992. Available from: <https://jamanetwork.com/journals/jamainternalmedicine/fullarticle/211417>
14. Gandelman K, Zhu T, Fahmi OA, et al. Unexpected Effect of Rifampin on the Pharmacokinetics of Linezolid: In Silico and In Vitro Approaches to Explain Its Mechanism. *J Clin Pharmacol* [Internet]. **2011**; 51(2):229–236. Available from: <http://doi.wiley.com/10.1177/0091270010366445>
15. Gebhart BC, Barker BC, Markewitz BA. Decreased serum linezolid levels in a critically ill patient receiving concomitant linezolid and rifampin. *Pharmacotherapy* [Internet]. *Pharmacotherapy*; **2007** [cited 2022 Oct 26]; 27(3):476–479. Available from: <https://pubmed.ncbi.nlm.nih.gov/17316160/>
16. Davis AG, Wasserman S, Maxebengula M, et al. Study protocol for a phase 2A trial of the safety and tolerability of increased dose rifampicin and adjunctive linezolid, with or without aspirin, for HIV-associated tuberculous meningitis [LASER-TBM]. *Wellcome open Res* [Internet]. The Wellcome Trust; **2021** [cited 2022 Jul 19]; 6:136. Available from: </pmc/articles/PMC8283551/>
17. Wasserman S, Davis A, Stek C, et al. Plasma pharmacokinetics of high-dose oral versus intravenous rifampicin in patients with tuberculous meningitis: a randomized controlled trial. *Antimicrob Agents Chemother*. **2021**; 65(8).
18. Garcia-Prats AJ, Schaaf HS, Draper HR, et al. Pharmacokinetics, optimal dosing, and safety of linezolid in children with multidrug-resistant tuberculosis: Combined data from two prospective observational studies. Denkinger CM, editor. *PLoS Med* [Internet]. Public Library of Science; **2019** [cited 2023 Mar 28]; 16(4):e1002789. Available from: <https://journals.plos.org/plosmedicine/article?id=10.1371/journal.pmed.1002789>
19. Diczfalusy U, Nylén H, Elander P, Bertilsson L. 4 $\beta$ -hydroxycholesterol, an endogenous marker of CYP3A4/5 activity in humans. *Br J Clin Pharmacol* [Internet]. Wiley-Blackwell; **2011** [cited 2022 Oct 13]; 71(2):183. Available from: </pmc/articles/PMC3040538/>

20. Anderson BJ, Holford NHG. Mechanism-based concepts of size and maturity in pharmacokinetics. *Annu Rev Pharmacol Toxicol*. **2008**; 48:303–332.
21. Janmahasatian S, Duffull SB, Ash S, Ward LC, Byrne NM, Green B. Quantification of Lean Bodyweight. *Clin Pharmacokinet*. **2005**; 44:1051–1065.
22. Beal SL. Ways to fit a PK model with some data below the quantification limit. *J Pharmacokinet Pharmacodyn*. **2001**; 28(5):481–504.
23. Cockcroft DW, Gault MH. Prediction of creatinine clearance from serum creatinine. *Nephron*. **1976**; 16(1):31–41.
24. Dosne A-G, Bergstrand M, Karlsson MO. An automated sampling importance resampling procedure for estimating parameter uncertainty. *J Pharmacokinet Pharmacodyn* [Internet]. Springer New York LLC; **2017**; 44(6):509–520. Available from: [https://www.ncbi.nlm.nih.gov/pmc/articles/PMC5686280/pdf/10928\\_2017\\_Article\\_9542.pdf](https://www.ncbi.nlm.nih.gov/pmc/articles/PMC5686280/pdf/10928_2017_Article_9542.pdf)
25. Deming WE. *Statistical adjustment of data*. Stat. Adjust. data. Oxford, England: Wiley; 1943.
26. Linnet K. Performance of Deming regression analysis in case of misspecified analytical error ratio in method comparison studies. *Clin Chem* [Internet]. **1998**; 44(5):1024–31. Available from: <http://www.ncbi.nlm.nih.gov/pubmed/9590376>
27. Kempker RR, Smith AGC, Avaliani T, et al. Cycloserine and Linezolid for Tuberculosis Meningitis: Pharmacokinetic Evidence of Potential Usefulness. *Clin Infect Dis* [Internet]. **2022**; 75(4):682–689. Available from: <https://doi.org/10.1093/cid/ciab992>
28. Viaggi B, Paolo A Di, Danesi R, et al. Linezolid in the central nervous system: Comparison between cerebrospinal fluid and plasma pharmacokinetics. <http://dx.doi.org/10.3109/003655482011582140> [Internet]. Taylor & Francis; **2011** [cited 2022 Apr 4]; 43(9):721–727. Available from: <https://www.tandfonline.com/doi/abs/10.3109/00365548.2011.582140>
29. Myrianthefs P, Markantonis SL, Vlachos K, et al. Serum and cerebrospinal fluid concentrations of linezolid in neurosurgical patients. *Antimicrob Agents Chemother*. **2006**; 50(12):3971–3976.
30. Lindbom L, Ribbing J, Jonsson EN. Perl-speaks-NONMEM (PsN)--a Perl module for NONMEM related programming. *Comput Methods Programs Biomed*. **2004**; 75(2):85–94.
31. Svensson EM, Dian S, Brake L Te, et al. Model-Based Meta-analysis of Rifampicin Exposure and Mortality in Indonesian Tuberculous Meningitis Trials. *Clin Infect Dis*. **2020**; 71(8):1817–1823.
32. Panjasawatwong N, Wattanakul T, Høglund RM, et al. Population Pharmacokinetic Properties of Antituberculosis Drugs in Vietnamese Children with Tuberculous Meningitis. *Antimicrob Agents Chemother* [Internet]. American Society for Microbiology; **2020** [cited 2021 Jun 7]; 65(1). Available from: </pmc/articles/PMC7927832/>
33. Williamson B, Dooley KE, Zhang Y, Back DJ, Owen A. Induction of influx and efflux transporters and cytochrome P450 3A4 in primary human hepatocytes by rifampin, rifabutin, and rifapentine. *Antimicrob Agents Chemother*. **2013**; 57(12):6366–6369.
34. Chen J, Raymond K. Roles of rifampicin in drug-drug interactions: Underlying molecular mechanisms involving the nuclear pregnane X receptor. *Ann Clin Microbiol Antimicrob* [Internet]. BioMed Central; **2006** [cited 2021 Feb 8]; 5(1):3. Available from: <http://ann-clinmicrob.biomedcentral.com/articles/10.1186/1476-0711-5-3>
35. Okazaki F, Tsuji Y, Seto Y, Ogami C, Yamamoto Y, To H. Effects of a rifampicin pre-treatment on linezolid pharmacokinetics. *PLoS One*. **2019**; 14(9):1–8.

36. Hashimoto S, Honda K, Fujita K, et al. Effect of coadministration of rifampicin on the pharmacokinetics of linezolid: clinical and animal studies. *J Pharm Heal Care Sci. Journal of Pharmaceutical Health Care and Sciences*; **2018**; 4(1):1–9.
37. Egle H, Trittler R, Kümmerer K, Lemmen SW. Linezolid and Rifampin: Drug Interaction Contrary to Expectations? *Clin Pharmacol Ther* [Internet]. John Wiley & Sons, Ltd; **2005** [cited 2022 Nov 3]; 77(5):451–453. Available from: <https://onlinelibrary.wiley.com/doi/full/10.1016/j.clpt.2005.01.020>
38. Imperial MZ, Nedelman JR, Conradie F, Savic RM. Proposed Linezolid Dosing Strategies to Minimize Adverse Events for Treatment of Extensively Drug-Resistant Tuberculosis. *Clin Infect Dis* [Internet]. **2022**; 74(10):1736–1747. Available from: <https://academic.oup.com/cid/article/74/10/1736/6380680>
39. Tietjen AK, Kroemer N, Cattaneo D, Baldelli S, Wicha SG. Population pharmacokinetics and target attainment analysis of linezolid in multidrug-resistant tuberculosis patients. *Br J Clin Pharmacol*. **2021**; (February):1–10.
40. Alghamdi WA, Al-Shaer MH, An G, et al. Population Pharmacokinetics of Linezolid in Tuberculosis Patients: Dosing Regimen Simulation and Target Attainment Analysis. *Antimicrob Agents Chemother* [Internet]. **2020**; 64(10). Available from: <http://doi.wiley.com/10.1177/0091270009337947>
41. Kamp J, Bolhuis MS, Tiberi S, et al. Simple strategy to assess linezolid exposure in patients with multi-drug-resistant and extensively-drug-resistant tuberculosis. *Int J Antimicrob Agents* [Internet]. Elsevier B.V.; **2017**; 49(6):688–694. Available from: <http://dx.doi.org/10.1016/j.ijantimicag.2017.01.017>
42. McGee B, Dietze R, Hadad DJ, et al. Population Pharmacokinetics of Linezolid in Adults with Pulmonary Tuberculosis. *Antimicrob Agents Chemother* [Internet]. **2009**; 53(9):3981–3984. Available from: <https://journals.asm.org/doi/10.1128/AAC.01378-08>
43. Meagher AK, Forrest A, Rayner CR, Birmingham MC, Schentag JJ. Population pharmacokinetics of linezolid in patients treated in a compassionate-use program. *Antimicrob Agents Chemother*. **2003**; 47(2):548–553.
44. Plock N, Buerger C, Joukhadar C, Kljucar S, Kloft C. Does linezolid inhibit its own metabolism? - Population pharmacokinetics as a tool to explain the observed nonlinearity in both healthy volunteers and septic patients. *Drug Metab Dispos*. **2007**; 35(10):1816–1823.
45. Mockeliunas L, Keutzer L, Sturkenboom MGG, et al. Model-Informed Precision Dosing of Linezolid in Patients with Drug-Resistant Tuberculosis. *Pharmaceutics* [Internet]. **2022**; 14(4):753. Available from: <https://www.mdpi.com/1999-4923/14/4/753>
46. Reiber H. Dynamics of brain-derived proteins in cerebrospinal fluid. *Clin Chim Acta*. **2001**; 310(2):173–186.
47. Reiber H. Proteins in cerebrospinal fluid and blood: Barriers, CSF flow rate and source-related dynamics. *Restor Neurol Neurosci*. **2003**; 21(3–4):79–96.
48. Harris PA, Taylor R, Thielke R, Payne J, Gonzalez N, Conde JG. Research electronic data capture (REDCap)-A metadata-driven methodology and workflow process for providing translational research informatics support. *J Biomed Inform* [Internet]. Elsevier Inc.; **2009**; 42(2):377–381. Available from: <http://dx.doi.org/10.1016/j.jbi.2008.08.010>

49. Harris PA, Taylor R, Minor BL, et al. The REDCap consortium: Building an international community of software platform partners. *J Biomed Inform* [Internet]. Elsevier; **2019**; 95(December 2018):103208. Available from: <https://doi.org/10.1016/j.jbi.2019.103208>

## TABLES

**Table 1 Clinical characteristics**

	Median (Min. – Max.) or No. (%)	
	Visit Day 3 (n = 30)	Visit Day 28 (n = 17)
Males	18 (60%)	11 (65%)
Age (years)	40 (27 – 56)	37 (27 – 51)
Weight (kg)	58 (30 – 96)	61 (37 – 81)
Height (m) <sup>a,c</sup>	1.61 (1.48 – 1.80)	1.61 (1.57 – 1.80)
Fat-free mass (kg) <sup>b,c</sup>	45 (30 – 59)	48 (32 – 60)
Serum creatinine (mmol/L)	61 (27 – 87)	50 (34 – 86)
4-beta hydroxy-cholesterol/cholesterol (molar ratio x10 <sup>-5</sup> ) <sup>d</sup>	1.48 (0.313 – 6.79)	1.90 (0.384 – 5.50)
Daily linezolid oral dose:		
1200 mg	30	10
600 mg	0	7
Duration of rifampicin treatment (days) <sup>e</sup>	5 (0 – 7)	30 (27 – 38)
CSF total protein (g/L)	1.46 (0.310 – 54.7)	0.750 (0.220 – 2.19)
CSF albumin (g/L)	3.32 (0.93 – 23.34)	4.47 (0.46 – 11.41)
CSF glucose (mmol/L)	2.9 (1.0 – 5.3)	3.2 (2.2 – 3.6)
Antiretroviral therapy (ART):		
Previous ART	11 (37%)	6 (35%)
ART Naïve	10 (33%)	5 (29%)
On ART	9 (30%)	6 (35%)
No. of participants concomitantly on:		
Tenofovir/Emtricitabine/Efavirenz	7	5
Abacavir/Lamivudine/Lopinavir	2	1

<sup>a</sup> Heights were missing for 18/30 (60%) participants and imputed based on sex and weight as outlined in the supplementary file.

<sup>b</sup> Fat-free mass was calculated based on sex, weight, and height according to the formula in Janmahasatian *et al.*<sup>21</sup>

<sup>c</sup> The median (min – max) values reported here are for the non-missing values (i.e., it does not include the imputed values).

<sup>d</sup> The ratio of 4 $\beta$ -OHC to cholesterol was missing in 4 and 3 participants on day 3 and day 28, respectively.

<sup>e</sup> This refers to the total number of days since the start of tuberculosis treatment, which was ~1-3 days before the recruitment into the study and start of the investigational treatment. Participants were on standard-dose (10 mg/kg) rifampicin when starting treatment and then switched to high-dose (35 mg/kg) rifampicin at the start of the study.

**Table 2 Final population pharmacokinetic parameter estimates for linezolid in plasma and lumbar cerebrospinal fluid**

Parameter	Estimate (95% confidence interval) <sup>a</sup> [%RSE] <sup>a</sup>
Maximal clearance, $CL_{max}$ (L/h) <sup>b</sup>	7.25 (6.09 – 8.86) [9.93]
Michaelis-Menten constant, $km$ (mg/L)	27.2 (16.0 – 46.4) [29.1]
Volume of distribution, $V$ (L) <sup>b</sup>	40.8 (37.9 – 43.6) [3.65]
Bioavailability, $F$ (.)	1 Fixed
Mean transit time, $MTT$ (h)	0.211 (0.112 – 0.342) [28.6]
No. of absorption transit compartments, $NN$ (.)	5.68 (2.36 – 11.8) [43.5]
Absorption rate constant, $ka$ (h <sup>-1</sup> )	1.21 (0.831 – 1.76) [19.6]
Proportional error plasma (%)	21.5 (18.8 – 24.7) [7.06]
Additive error plasma (mg/L) <sup>d</sup>	0.173 (0.0379 – 0.355) [47.1]
Between-subject variability (BSV) in $CL_{max}$ (%)	9.60 (3.44 – 13.9) [51.9]
Between-visit variability (BVV) in $CL_{max}$ (%)	20.3 (15.3 – 26.9) [30.7]
Between-occasion variability (BOV) in $ka$ (%)	87.9 (66.4 – 110) [25.9]
BOV in $MTT$ (%)	110 (75.8 - 144) [32.8]
Equilibration rate constant to CSF, $k_{plasma-CSF}$ (h <sup>-1</sup> ) <sup>e</sup>	0.198 (0.0849 – 0.340) [33.7]
Maximal pseudo-partition coefficient to CSF, $PPC_{max}$ (.)	0.365 (0.238 – 0.566) [23.2]
CSF protein at which $PPC_{max}$ is reached, $CSF\ protein_{max}$ (mg/mL) <sup>f</sup>	1.18 (0.730 – 1.90) [24.4]
Proportional error CSF (%)	91.5 (63.3 – 151) [23.4]
Additive error CSF (mg/L) <sup>d</sup>	0.02 Fixed

<sup>a</sup> Values in parentheses are the 95% confidence intervals and those in square brackets are the % relative standard errors, both computed with sampling importance resampling (SIR) on the final model.

<sup>b</sup> The values of  $CL_{max}$  and  $V$  were allometrically scaled, so the typical values reported here refer to the typical participant, i.e. a median FFM of 45 kg.

<sup>d</sup> The estimate of the additive component of the error was not significantly different from its lower boundary of 20% of LLOQ, so it was fixed to this value.

<sup>e</sup> Corresponds to an equilibration half-life of 3.5 (2.04 – 8.16) h

<sup>f</sup> For CSF protein <  $CSF\ protein_{max}$  (i.e., the breakpoint):  $PPC_i = PPC_{max} \cdot (slope \cdot (CSF\ protein - breakpoint))$ , where the *breakpoint* was estimated to be 1.18 mg/mL, and the *slope* was calculated to be 0.847 from the following equation:  $slope = (amplitude - intercept) / (breakpoint - 0)$ , where the *intercept* and *amplitude* were fixed to 0 and 1, respectively. For CSF protein  $\geq CSF\ protein_{max}$ :  $PPC_i = PPC_{max}$ . The PPC-CSF protein relationship is depicted in **Figure 2**, and more details are provided in the supplementary file.

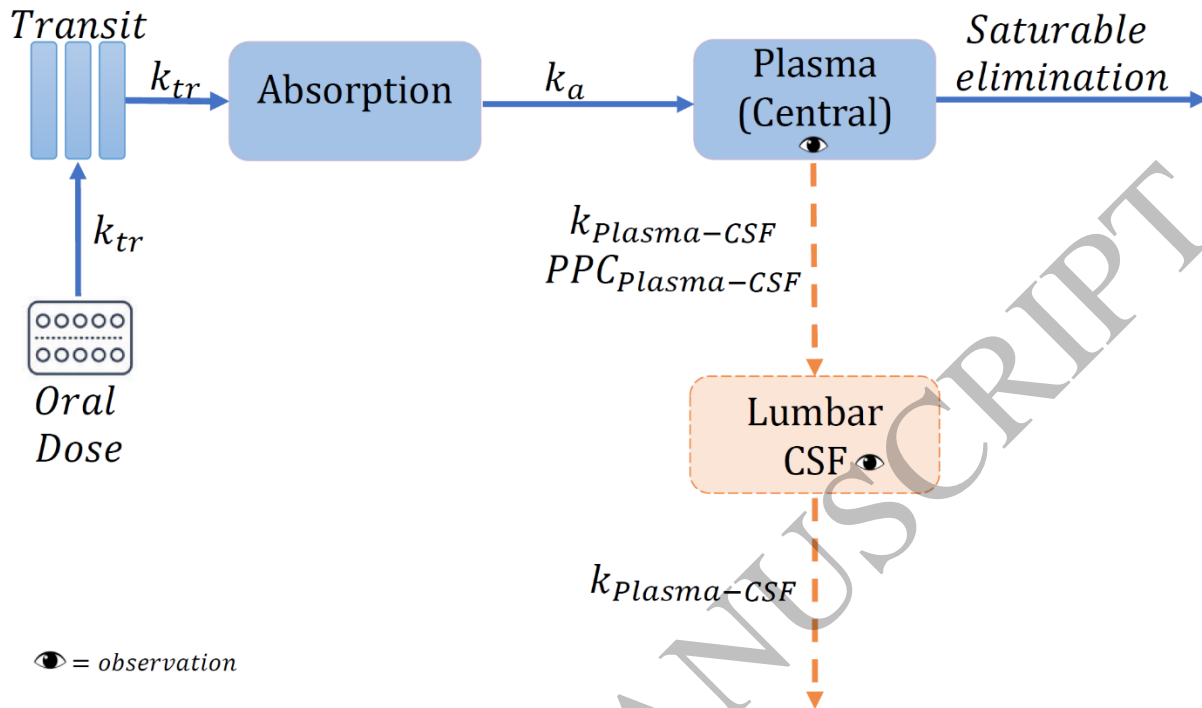
**Table 3 Linezolid model-derived area under the curve for 24 hours and concentrations at 24 hours post-dose**

	Median (Min. – Max.)			
	Plasma		Cerebrospinal fluid	
Daily oral dose	1200 mg (n = 40)	600 mg (n = 7)	1200 mg (n = 40)	600 mg (n = 7)
$AUC_{0-24h}$ (mg · h/L)	278 (87.3 - 762)	93.7 (66.7 - 167)	81.6 (19.7 - 234)	24.0 (6.55 - 56.8)
$C_{24}$ (mg/L)	1.69 (0.154 - 13.5)	0.406 (0.0614 - 1.67)	1.32 (0.327 - 6.48)	0.369 (0.0495 - 1.02)

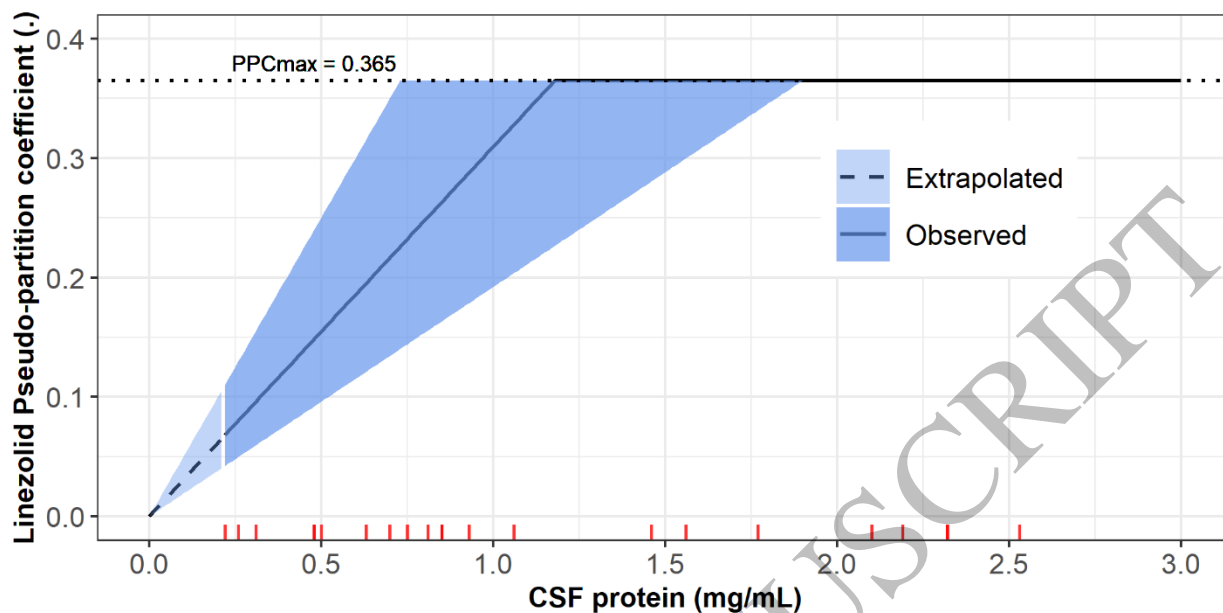
## FIGURES

**Figure 1:** Schematic representation of the final model.  $k_{tr}$  is the rate constant for the drug passage through the transit compartments,  $k_{Plasma-CSF}$ , equilibration rate constant plasma-cerebrospinal fluid (CSF) which describes how soon the change in plasma is reflected in the CSF;  $PPC_{Plasma-CSF}$ , the pseudo-partition coefficient which represents the ratio of drug in CSF to the plasma.

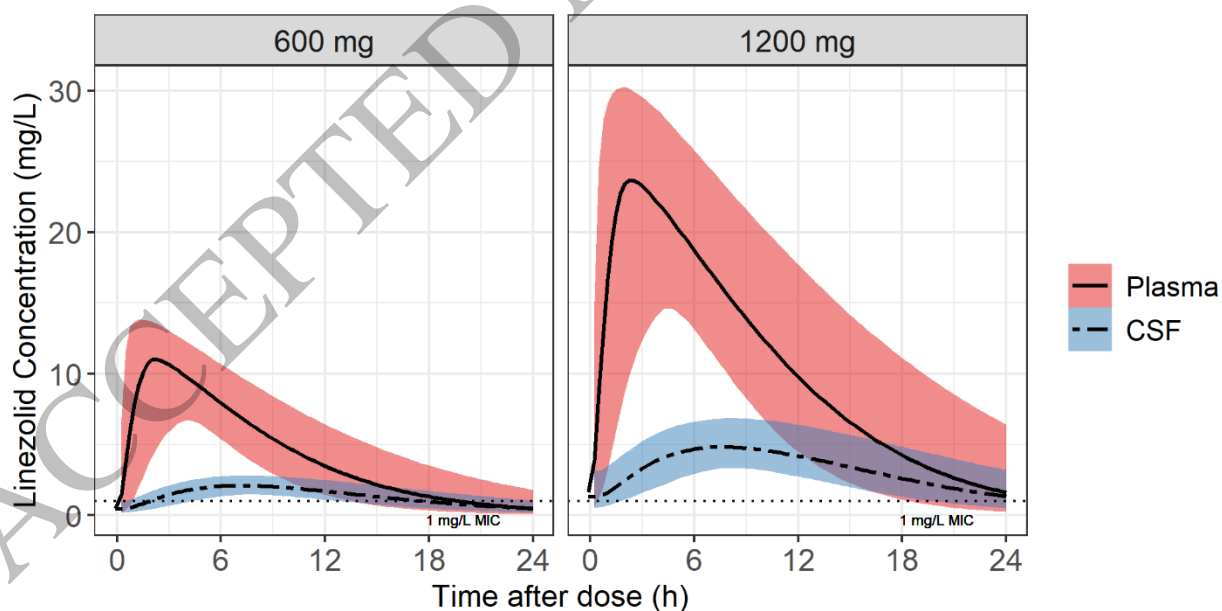




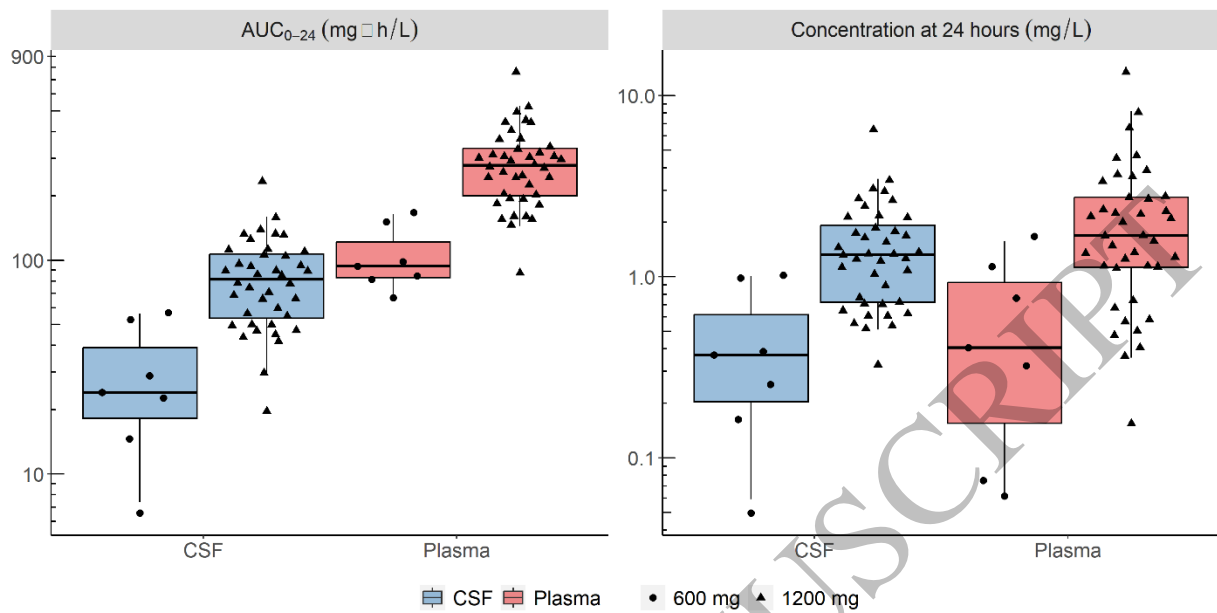
**Figure 2:** The relationship of *PPC* vs the CSF protein level using the piece-wise (broken-stick) function. The solid line represents the median and the shaded areas represent the uncertainty around the estimates of the breakpoint (the maximal CSF protein value at which *PPC<sub>max</sub>* is reached) and the calculated slope. The dashed line depicts the extrapolated part of the *PPC*-CSF protein relationship for CSF protein values outside the range observed in the study cohort (The lowest observed value was 0.22 mg/mL). The red ticks represent the values of CSF protein observed in our cohort (CSF protein values above 3 mg/mL were truncated for better figure visibility. Some red ticks are overlapping because there are some duplicated CSF protein values).



**Figure 3:** Simulated typical concentration-time profiles for plasma and cerebrospinal fluid (CSF) for the 1200 mg and 600 mg oral daily dose of linezolid. The solid and dashed lines represent the median for the plasma and CSF, respectively and the shaded areas represent the 90% confidence intervals. The horizontal dotted line indicates the wild-type minimum inhibitory concentration (MIC) value of linezolid for *M. tuberculosis*.



**Figure 4:** Box and whisker plots showing the secondary model-derived exposure parameters,  $AUC_{0-24h}$  and concentration at 24 hours post-dose ( $C_{24h}$ ) stratified by dose. The boxes represent inter-quartile range, while whiskers are the 2.5<sup>th</sup> and 97.5<sup>th</sup> percentiles. The dots represent individual values ( $n = 7$  for 600 mg and 40 for 1200 mg of which 30 on day 3 and 10 on day 28).



ACCEPTED MANUSCRIPT